

3. Boyce, C. K. & Knoll, A. H. Evolution of developmental potential and the multiple independent origin of leaves in Paleozoic vascular plants. *Paleobiology* **28**, 70–100 (2002).
4. Kenrick, P. & Crane, P. R. *The Origin and Early Diversification of Land Plants: A Cladistic Study* (Smithsonian Institution Press, London, 1997).
5. Jackson, D., Veit, B. & Hake, S. Expression of maize *Knotted1* related homeobox genes in the shoot apical meristem predicts patterns of morphogenesis in the vegetative shoot. *Development* **120**, 404–413 (1994).
6. Lincoln, C., Long, J., Yamaguchi, J., Serikawa, K. & Hake, S. A. *Knotted1*-like homeobox gene in *Arabidopsis* is expressed in the vegetative meristem and dramatically alters leaf morphology when overexpressed in transgenic plants. *Plant Cell* **6**, 1859–1876 (1994).
7. Nishimura, A., Tamaoki, M., Sato, Y. & Matsuoka, M. The expression of tobacco *Knotted1*-type class I homeobox genes correspond to regions predicted by the cytohistological zonation model. *Plant J.* **18**, 337–347 (1999).
8. Long, J. A., Moan, E. I., Medford, J. I. & Barton, M. K. A member of the KNOTTED class of homeodomain proteins encoded by the *STM* gene of *Arabidopsis*. *Nature* **379**, 66–69 (1996).
9. Sentoku, N. *et al.* Regional expression of the rice *KN1*-type homeobox gene family during embryo, shoot and flower development. *Plant Cell* **11**, 1651–1663 (1999).
10. Hofer, J. M., Gourlay, C. W., Michael, A. & Ellis, T. H. Expression of a class I *Knotted1*-like homeobox gene is down-regulated in pea compound leaf primordia. *Plant Mol. Biol.* **45**, 387–398 (2001).
11. Hareven, D., Gutfinger, T., Parnis, A., Eshed, Y. & Lifschitz, E. The making of a compound leaf: genetic manipulation of leaf architecture in tomato. *Cell* **84**, 735–744 (1996).
12. Muller, J. *et al.* *In vitro* interactions between barley TALE homeodomain proteins suggest a role for protein-protein associations in the regulation of *Knox* gene function. *Plant J.* **27**, 13–23 (2001).
13. Byrne, M. E. *et al.* ASYMMETRIC LEAVES1 mediates leaf patterning and stem cell function in *Arabidopsis*. *Nature* **408**, 967–971 (2000).
14. Schneeberger, R., Tsiantis, M., Freeling, M. & Langdale, J. A. The *rough sheath2* gene negatively regulates homeobox gene expression during maize leaf development. *Development* **125**, 2857–2865 (1998).
15. Tsiantis, M., Schneeberger, R., Golz, J. F., Freeling, M. & Langdale, J. A. The maize *rough sheath2* gene and leaf development programs in monocot and dicot plants. *Science* **284**, 154–156 (1999).
16. Timmermans, M. C. P., Hudson, A., Becraft, P. W. & Nelson, T. ROUGH SHEATH2: A myb protein that represses *Knox* homeobox genes in maize lateral organ primordia. *Science* **284**, 151–153 (1999).
17. Smith, L. G., Greene, B., Veit, B. & Hake, S. A dominant mutation in the maize homeobox gene, *Knotted-1*, causes its ectopic expression in leaf cells with altered fates. *Development* **116**, 21–30 (1992).
18. McHale, N. A. & Koning, R. E. PHANTASTICA regulates development of the adaxial mesophyll in *Nicotiana* leaves. *Plant Cell* **16**, 1251–1262 (2004).
19. Wikstrom, N., Savolainen, V. & Chase, M. W. Evolution of the angiosperms: calibrating the family tree. *Proc. R. Soc. Lond. B* **268**, 2211–2220 (2001).
20. Tsiantis, M. & Hay, A. Comparative plant development: the time of the leaf? *Nature Rev. Genet.* **4**, 169–180 (2003).
21. Steeves, T. A. & Sussex, I. M. Studies on the development of excised leaves in sterile culture. *Am. J. Bot.* **44**, 665–673 (1957).
22. Bierhorst, D. W. On the stem apex, leaf initiation and early leaf ontogeny in filiclean ferns. *Am. J. Bot.* **64**, 125–152 (1977).
23. Bharathan, G. *et al.* Homologies in leaf form inferred from *KNOX1* gene expression during development. *Science* **296**, 1858–1860 (2002).
24. Kim, M., McCormick, S., Timmermans, M. & Sinha, N. The expression domain of PHANTASTICA determines leaflet placement in compound leaves. *Nature* **424**, 438–443 (2003).
25. Kim, M. *et al.* Reduced leaf complexity in tomato wiry mutants suggests a role for PHAN and KNOX genes in generating compound leaves. *Development* **130**, 4405–4415 (2003).
26. Theodoris, G., Inada, N. & Freeling, M. Conservation and molecular dissection of ROUGH SHEATH2 and ASYMMETRIC LEAVES1 function in leaf development. *Proc. Natl Acad. Sci. USA* **100**, 6837–6842 (2003).
27. Pautot, V. *et al.* *KNAT2*: evidence for a link between *Knotted*-like genes and carpel development. *Plant Cell* **13**, 1719–1734 (2001).
28. Golz, J. F., Keck, E. J. & Hudson, A. Spontaneous mutations in *KNOX* genes give rise to a novel floral structure in antirrhinum. *Curr. Biol.* **12**, 515–522 (2002).
29. Parnis, A. *et al.* The dominant developmental mutants of tomato, *Mouse-Ear* and *Curl*, are associated with distinct modes of abnormal transcriptional regulation of a *Knotted* gene. *Plant Cell* **9**, 2143–2158 (1997).
30. Janssen, B.-J., Lund, L. & Sinha, N. Overexpression of a homeobox gene *LeT6* reveals indeterminate features in the tomato compound leaf. *Plant Physiol.* **117**, 771–786 (1998).

Supplementary Information accompanies the paper on [www.nature.com/nature](http://www.nature.com/nature).

**Acknowledgements** We thank D. Stork for technical help; C. Hammond and T. Gardner for help during their undergraduate degrees (funded by the Wellcome Trust and a Nuffield Bursary, respectively); M. Tsiantis and G. Theodoris for *rs2* fusion constructs; M. Tsiantis and M. Knight for criticizing our manuscript; M. Tsiantis, D. Barker and the Oxford Systematics Discussion Group for discussions; and J. Hofer, A. Hudson and N. McHale for the use of unpublished data presented in Fig. 3. D.L.A. was the recipient of a Sainsbury PhD studentship. The work was funded by a grant to J.A.L. and R.W.S. from the Biotechnology and Biological Sciences Research Council.

**Competing interests statement** The authors declare that they have no competing financial interests.

**Correspondence** and requests for materials should be addressed to J.A.L. ([jane.langdale@plants.ox.ac.uk](mailto:jane.langdale@plants.ox.ac.uk)). Sequences have been deposited in GenBank as follows: *SkKNOX1* (AY667449), *SkKNOX2* (AY667450), *SkKNOX3* (AY667451), *SkARPI* (AY667452) and *SvARPI* (AY667453).

## Leptin regulation of bone resorption by the sympathetic nervous system and CART

Florent Elefteriou<sup>1,2,3</sup>, Jong Deok Ahn<sup>1,2</sup>, Shu Takeda<sup>1,2,4,5</sup>, Michael Starbuck<sup>1,2</sup>, Xiangli Yang<sup>1,2</sup>, Xiyun Liu<sup>1,2</sup>, Hisataka Kondo<sup>5,6</sup>, William G. Richards<sup>7</sup>, Tony W. Bannion<sup>7</sup>, Masaki Noda<sup>5,6</sup>, Karine Clement<sup>8</sup>, Christian Vaisse<sup>9</sup> & Gerard Karsenty<sup>1,2,3</sup>

<sup>1</sup>Department of Molecular and Human Genetics, <sup>2</sup>Bone Disease Program of Texas, <sup>3</sup>Children's Nutrition Research Center, Baylor College of Medicine, Houston, Texas 77030, USA

<sup>4</sup>Department of Orthopedics, <sup>5</sup>Center of Excellence Program for Frontier Research on Molecular Destruction and Reconstruction of Tooth and Bone, <sup>6</sup>Department of Molecular Pharmacology, Medical Research Institute, Tokyo Medical and Dental University, Tokyo 101-0062, Japan

<sup>7</sup>Amgen Inc., Neuroscience, Thousand Oaks, California 91320, USA

<sup>8</sup>INSERM Avenir team—University Paris 6, EA3502, and CHRU Pitié Salpêtrière, Hôtel-Dieu Nutrition Department, F-75004 Paris, France

<sup>9</sup>Diabetes Center and Department of Medicine, University of California San Francisco, San Francisco, California 94143, USA

Bone remodelling, the mechanism by which vertebrates regulate bone mass, comprises two phases, namely resorption by osteoclasts and formation by osteoblasts; osteoblasts are multifunctional cells also controlling osteoclast differentiation. Sympathetic signalling via  $\beta$ 2-adrenergic receptors (*Adrb2*) present on osteoblasts controls bone formation downstream of leptin<sup>1</sup>. Here we show, by analysing *Adrb2*-deficient mice, that the sympathetic nervous system favours bone resorption by increasing expression in osteoblast progenitor cells of the osteoclast differentiation factor *Rankl*. This sympathetic function requires phosphorylation (by protein kinase A) of ATF4, a cell-specific CREB-related transcription factor essential for osteoblast differentiation and function<sup>2</sup>. That bone resorption cannot increase in gonadectomized *Adrb2*-deficient mice highlights the biological importance of this regulation, but also contrasts sharply with the increase in bone resorption characterizing another hypogonadic mouse with low sympathetic tone, the *ob/ob* mouse<sup>3</sup>. This discrepancy is explained, in part, by the fact that CART ('cocaine amphetamine regulated transcript'), a neuropeptide whose expression is controlled by leptin and nearly abolished in *ob/ob* mice<sup>4</sup>, inhibits bone resorption by modulating *Rankl* expression. Our study establishes that leptin-regulated neural pathways control both aspects of bone remodelling, and demonstrates that integrity of sympathetic signalling is necessary for the increase in bone resorption caused by gonadal failure.

Leptin antiosteogenic function is mediated by the sympathetic nervous system (SNS) acting through *Adrb2*, the only adrenergic receptor expressed in osteoblasts<sup>1</sup> (Supplementary Fig. 1). If both arms of bone remodelling are regulated by similar mechanisms, these results imply that bone resorption (BR) is controlled by neural means. To test this hypothesis, we used mutant mice in which pathways acting downstream of leptin signalling were disrupted.

*Adrb2*<sup>-/-</sup> mice have normal body weight and fat pad weight<sup>5</sup>, and none of the endocrine abnormalities observed in mice lacking leptin (*ob/ob*) or noradrenaline (*Dopamine- $\beta$ -hydroxylase* (*Dbh*)<sup>-/-</sup> mice, Fig. 1a)<sup>6,7</sup>. Analyses of vertebrae and long bones revealed two unanticipated features in 6-month-old male and female *Adrb2*<sup>-/-</sup> mice. First, *Adrb2*<sup>-/-</sup> mice had a more severe high bone mass phenotype (HBM) than *ob/ob* or wild-type (WT) mice receiving  $\beta$ -blockers<sup>1,3</sup> (Fig. 1b, c). Illustrating the importance of sympathetic signalling in bone remodelling, this HBM also affected *Adrb2*<sup>+/-</sup>

mice yet *Adrb2*<sup>+/-</sup> osteoblasts do transduce a signal through *Adrb2* following treatment with isoproterenol (ISO), a surrogate of sympathetic signalling (Fig. 1b, d). This HBM was not observed in mice lacking *Adrb1* (Supplementary Fig. 2), indicating that *Adrb2*<sup>-/-</sup> mice are the best model to elucidate how sympathetic signalling in bone cells regulates bone mass. That long-term leptin intracerebroventricular (ICV) infusion did not reduce bone mass of *Adrb2*<sup>-/-</sup> mice established that SNS integrity is necessary for leptin antiosteogenic function (Fig. 1e).

To determine whether *Adrb2*<sup>-/-</sup> mice HBM involves bone cell-autonomous mechanisms, we performed transplantation of non-adherent bone marrow cells (BMCs)<sup>8</sup>. Transplantation of WT BMC into  $\gamma$ -irradiated *Adrb2*<sup>-/-</sup> mice normalized bone formation parameters; conversely, transplantation of *Adrb2*<sup>-/-</sup> BMC into  $\gamma$ -irradiated WT mice significantly increased bone formation (Fig. 1f). Polymerase chain reaction (PCR) analysis of *in vitro* differentiated osteoblastic colonies showed the presence of WT or *Adrb2*<sup>-/-</sup> osteoblasts in *Adrb2*<sup>-/-</sup> or WT  $\gamma$ -irradiated mice,

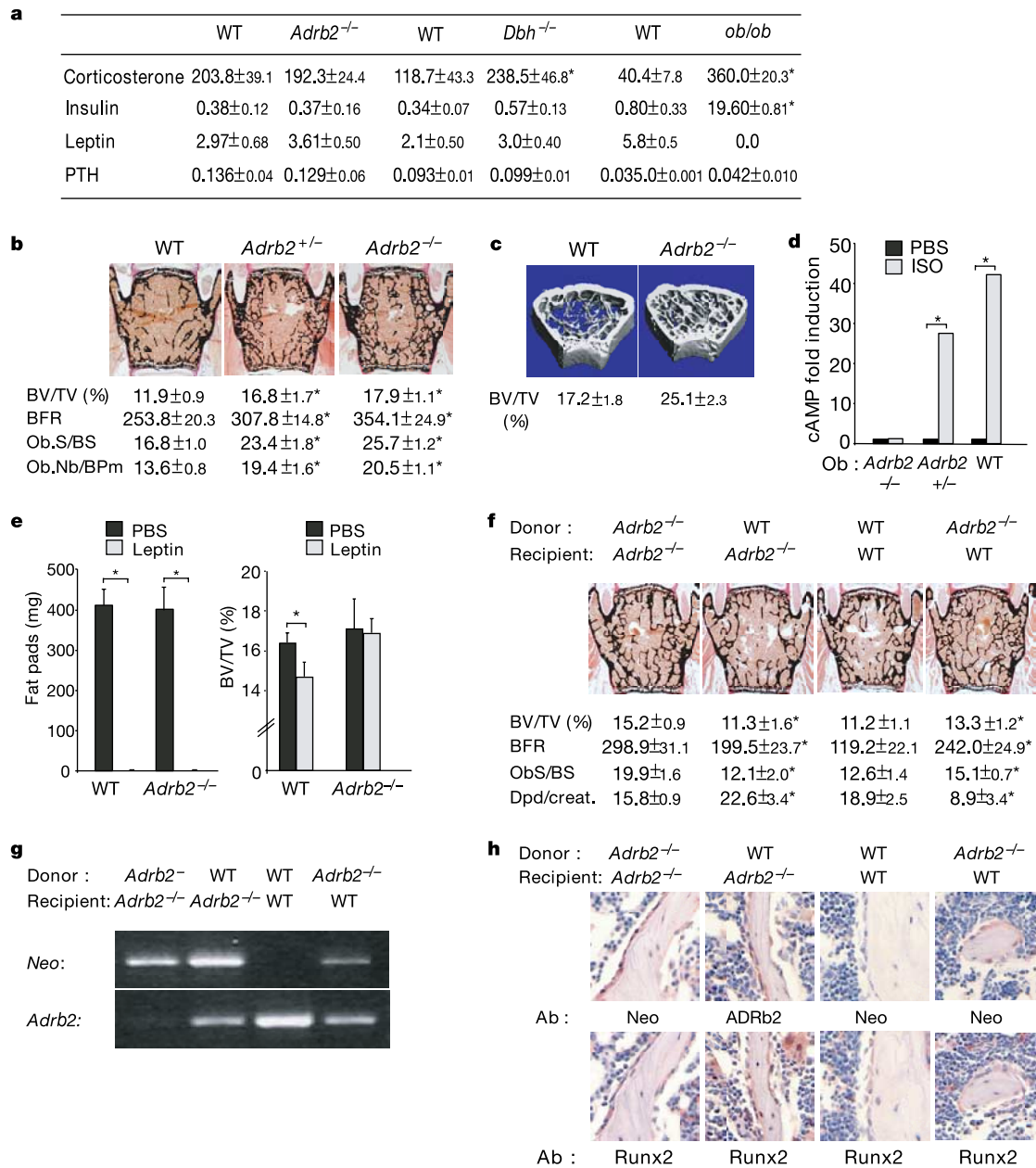


**Figure 1** Increased bone formation in *Adrb2*-deficient mice. **a**, Hormonal measurements (ng ml<sup>-1</sup>, mean + s.e.m) in 6- (*Adrb2*<sup>-/-</sup> and *Dbh*<sup>-/-</sup>) and 3-month-old (*ob/ob*) mice. Differences in ages and genetic backgrounds explain different hormonal levels. **b**, Bone volume/tissue volume (BV/TV, %), bone formation rate (BFR,  $\mu\text{m}^3 \mu\text{m}^{-2} \text{yr}^{-1}$ ), osteoblast surface/bone surface (Ob.S/BS) and osteoblast number/bone perimeter (Ob.Nb/BPm) in 6-month-old mice (mean + s.e.m). **c**,  $\mu\text{CT}$  analysis of 6-month-old distal femurs. **d**, cAMP production in phosphate buffered saline (PBS) and isoproterenol (ISO)-treated

osteoblasts (Ob). **e**, Fat pad weight and BV/TV following leptin ICV infusion. **f**, Formation and resorption parameters following transplantations. Comparison is between the same recipient genotype (mean + s.e.m). **g**, PCR analysis of transplantation efficiency using Neomycin (Neo) and *Adrb2*-specific primers. **h**, Immunocytochemical detection of Neomycin<sup>+</sup>, Runx2<sup>+</sup> and *Adrb2*<sup>+</sup> osteoblasts in WT and *Adrb2*<sup>-/-</sup> bones following transplantation. Error bars, mean + s.e.m. \*Statistically significant.

respectively (Fig. 1g and data not shown). Immunocytochemistry analysis showed Neomycin<sup>+</sup>, Runx2<sup>+</sup> osteoblasts in WT mice transplanted with *Adrb2*<sup>-/-</sup> BMCs and *Adrb2*<sup>+</sup>, Runx2<sup>+</sup>, Neomycin<sup>-</sup> osteoblasts in *Adrb2*<sup>-/-</sup> mice transplanted with WT BMCs (Fig. 1h). Thus the SNS controls bone mass by acting, at least in part, on cells of the osteoblast lineage.

Further cellular analysis of *Adrb2*<sup>-/-</sup> mice revealed a second unanticipated feature. Besides the expected increase in bone formation parameters<sup>1</sup> (Fig. 1b), there was, in all bones analysed, a significant decrease in BR parameters, including a decrease in number of tartrate-resistant acid phosphatase (TRAP)-positive multi-nucleated osteoclasts, indicative of a defect in osteoclast differentiation, and a decrease in urinary elimination of deoxy-pyridinoline (Dpd), a marker of osteoclast function (Fig. 2a). This was unexpected, because *ob/ob* or  $\beta$ -blocker-treated WT mice<sup>1</sup> have high and normal BR, respectively (Fig. 2b and data not shown). A decrease in Dpd urinary elimination was also observed in WT mice transplanted with *Adrb2*<sup>-/-</sup> BMC, while WT BMC transplantation into *Adrb2*<sup>-/-</sup> mice increased it (Fig. 1f). These BR abnormalities

were not corrected by leptin ICV infusion, indicating that leptin signalling regulates BR via the SNS (Fig. 2b).

To determine whether sympathetic signalling acts on osteoclast, we cultured bone marrow macrophages (BMMs) in the presence of RANKL, an osteoclast differentiation factor, and M-CSF, an osteoclast proliferation factor<sup>9,10</sup>. WT or *Adrb2*<sup>-/-</sup> BMMs differentiated equally well into osteoclasts at each RANKL/M-CSF dose tested (Fig. 2c), and ISO did not hamper generation of osteoclasts (Supplementary Fig. 3). *Adrb2* inactivation did not alter the ability of osteoclasts to generate resorption pits on dentine slices, and ISO did not increase cAMP production in osteoclasts (Fig. 2d-e).

Next we asked whether the SNS affects BR by acting in osteoblasts, a cell type controlling osteoclast differentiation<sup>9</sup>. ISO enhanced generation of osteoclasts when WT, but not *Adrb2*<sup>-/-</sup>, osteoblasts were co-cultured with WT BMMs (Fig. 2f). Moreover, ISO treatment of WT, but not *Adrb2*<sup>-/-</sup>, osteoblasts increased expression of *Rankl* (a secreted osteoclast differentiation factor) to a greater extent than did parathyroid hormone (PTH), a hormone

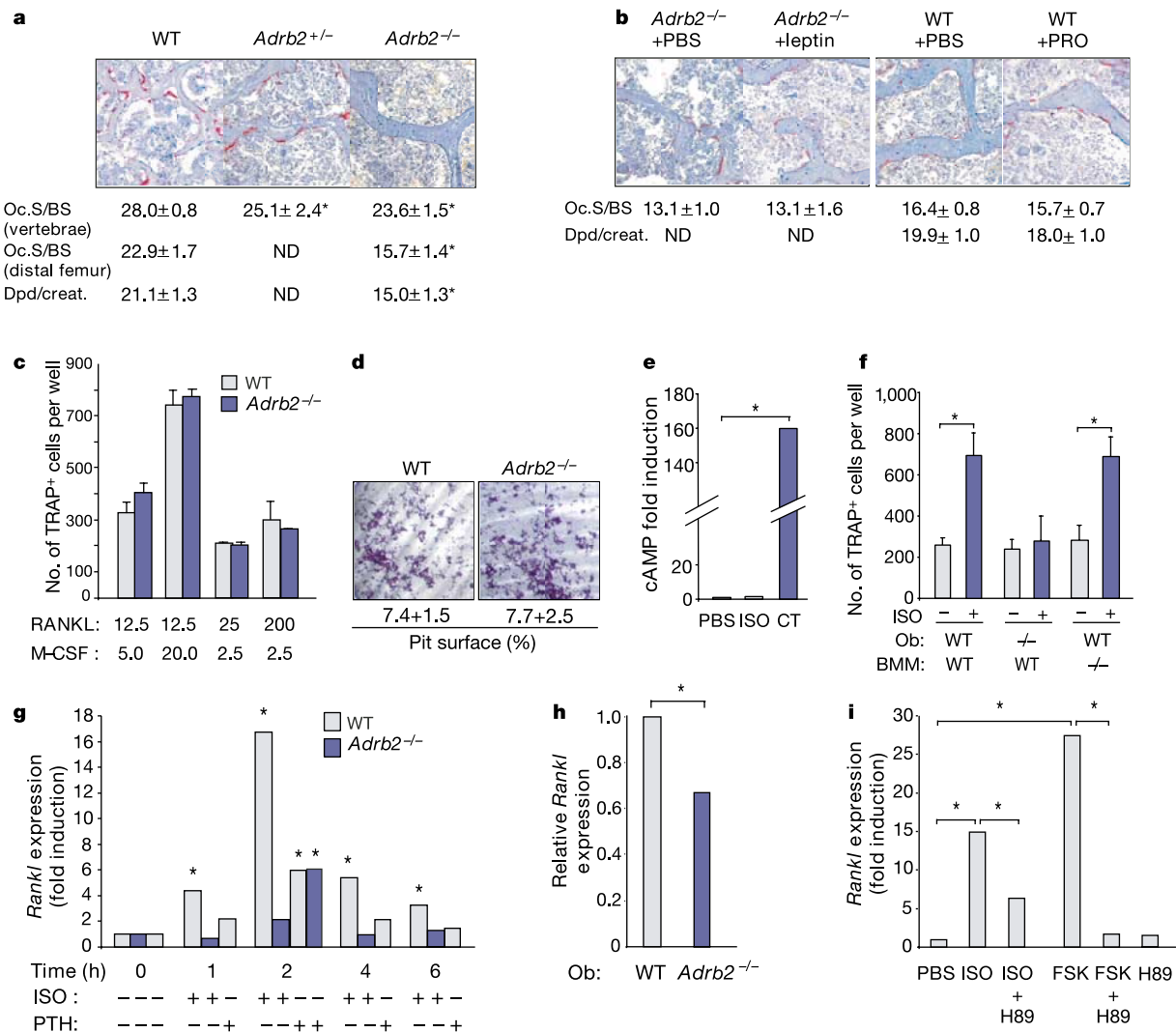


**Figure 2** Sympathetic signalling in osteoblasts regulates BR. **a, b**, Osteoclast surface/ bone surface and Dpd/creatinine in 6-month-old mice; **b**, following leptin ICV or propranolol (PRO) treatment. ND, not determined. **c**, *In vitro* differentiation of WT and *Adrb2*<sup>-/-</sup> BMMs with limiting amounts of RANKL and M-CSF (ng ml<sup>-1</sup>). **d**, WT and *Adrb2*<sup>-/-</sup> osteoclasts generate resorption pits equally well. **e**, Calcitonin, not ISO,

induces cAMP production in osteoclasts. **f**, Number of TRAP<sup>+</sup> cells following co-culture of osteoblasts and BMMs in the presence of ISO. **g-i**, Real-time PCR. ISO induces *Rankl* expression in WT not *Adrb2*<sup>-/-</sup> osteoblasts. *Rankl* expression is decreased in *Adrb2*<sup>-/-</sup> osteoblasts and PKA is required for ISO induction of *Rankl* expression (*n* = 3 per experiment). Error bars, mean + s.e.m. \*Statistically significant.

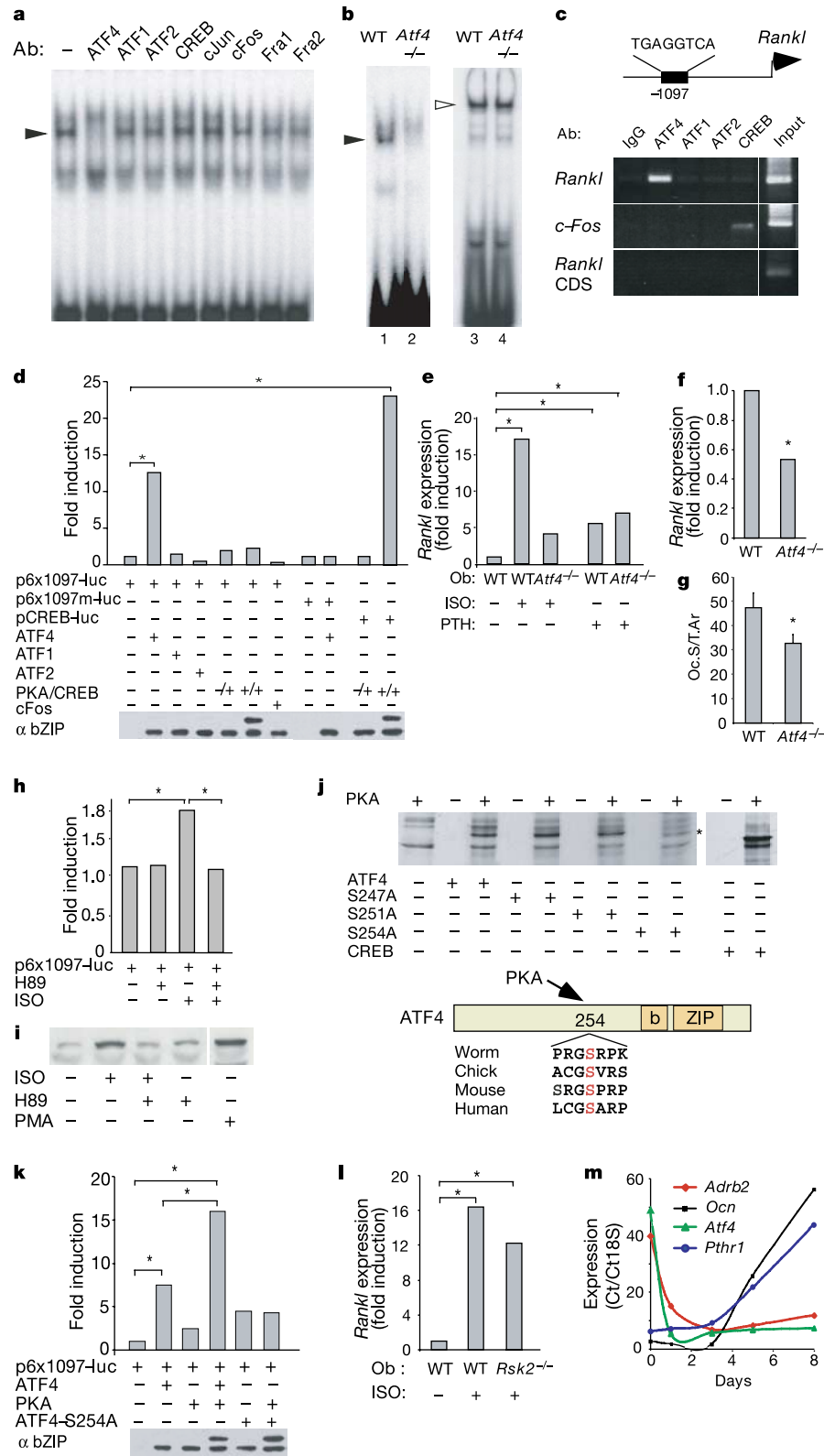


**Figure 3** Sympathetic regulation of *Rankl* expression. **a**, EMSA: ATF4 antibody prevented formation of protein–DNA complex (filled arrow) on *Rankl* promoter CRE site. **b**, WT (1) but not *Atf4*<sup>-/-</sup> (2) osteoblast nuclear extracts bind to -1097<sup>*Rankl*</sup>. Sp1 (open arrow) served as control (3, 4). **c**, ChIP: ATF4 binds to -1097<sup>*Rankl*</sup> but not to *Rankl* coding sequence (CDS). **d**, DNA cotransfections in COS cells using multimers of WT or mutant -1097<sup>*Rankl*</sup> (p6x1097-*luc*) or pCREB-*luc* and indicated expression vectors. **e**, Real-time PCR. *Rankl* induction by ISO but not by PTH is blunted in *Atf4*<sup>-/-</sup> osteoblasts. **f, g**, Decreased *Rankl* expression and *Oc.S/Tar* in absence of *Atf4*<sup>-/-</sup>. **h**, ISO increased

ATF4 transactivation activity, H89 inhibited it, in ROS 17/2.8 cells. **i**, Phospho-<sup>254</sup>ATF4 western blot. H89 inhibits ATF4 phosphorylation following ISO treatment. **j**, *In vitro* kinase assay. ATF4 is phosphorylated by PKA on serine 254 (asterisk). CREB served as positive control. **k**, DNA cotransfection assays in COS cells. PKA increases ATF4 transactivation activity through serine 254. **l, m**, Real-time PCR. ISO induces *Rankl* expression in *Rsk2*<sup>-/-</sup> osteoblasts. *Adrb2*, *Pthr*, *Atf4* and *Osteocalcin (Ocn)* expression during osteoblast differentiation. Bottom line of **d** and **k** shows western blots of transfected proteins. \*Statistically significant.

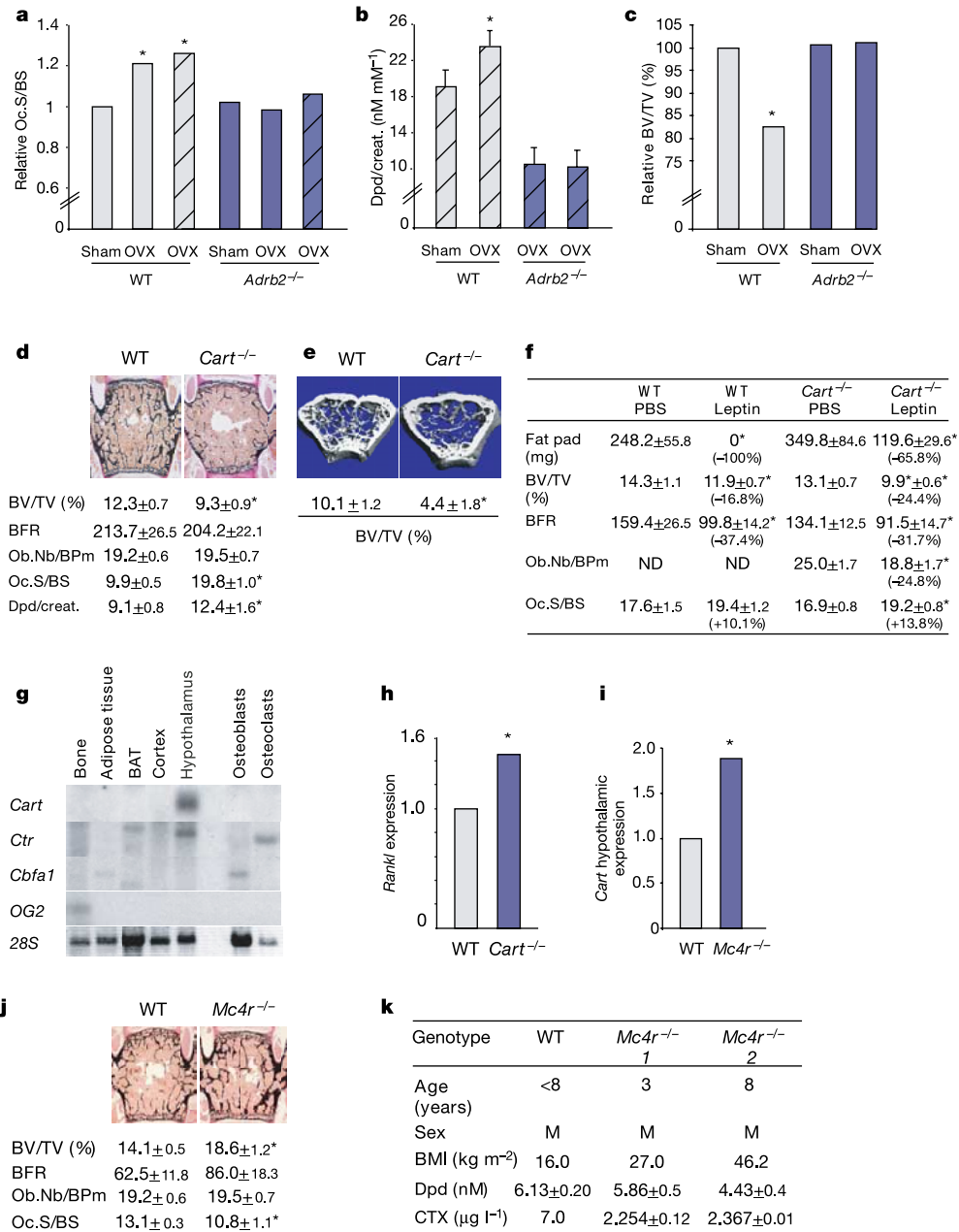


**Figure 4** SNS and CART antagonistic functions. **a-c**, Relative Oc.S/BS, urinary Dpd and BV/TV in WT and *Adrb2*<sup>-/-</sup> mice ovariectomized (OVX) for 4 or 12 weeks (plain or hatched bars). \**P* < 0.05 versus WT sham littermates. **d**, BV/TV, formation and resorption parameters in 6-month-old *Cart*<sup>-/-</sup> mice. **e**,  $\mu$ CT analysis of 6 month-old femurs. **f**, Leptin ICV infusion in WT and *Cart*<sup>-/-</sup> mice. *Cart* deletion enhances leptin antiosteogenic and proresorptive functions. **g**, Northern blots. *Cart* is not expressed in

bone cells. **h,i**, Real-time PCR. Increased *Rankl* and *Cart* expression in *Cart*<sup>-/-</sup> and *Mc4r*<sup>-/-</sup> bones and hypothalami. **j**, Increased BV/TV, normal bone formation, decreased bone resorption in 6-month-old *Mc4r*<sup>-/-</sup> mice. **k**, Serum Dpd and crosslaps CTX are decreased in MC4R-deficient patients. Error bars, mean + s.e.m. BMI, body mass index.

that upregulates *Rankl* expression in both WT<sup>9</sup> and *Adrb2*<sup>-/-</sup> osteoblasts (Fig. 2g). Accordingly, *Rankl* expression was decreased in *Adrb2*<sup>-/-</sup> osteoblasts (Fig. 2h). ISO did not affect expression of *Osteoprotegerin* (a *Rankl* decoy receptor) or of other cytokines (Supplementary Fig. 4).

ISO induction of *Rankl* was blunted by a PKA inhibitor, suggesting that CREB mediates it (Fig. 2i). A CREB-responsive element is present in *Rankl* promoter at -1097, and a protein-DNA complex formed upon incubation of osteoblast nuclear extracts

with this element in electrophoretic mobility shift assay (EMSA) (Fig. 3a). Surprisingly, this protein-DNA complex was not affected by an antibody against CREB but was abolished by an antibody against ATF4, an osteoblast-specific CREB/ATF family member essential for osteoblast function<sup>2</sup>. Several lines of evidence demonstrated that ATF4 mediates sympathetic regulation of *Rankl* expression in osteoblasts. First, in EMSA, this protein-DNA complex did not form when nuclear extracts of *Atf4*<sup>-/-</sup> osteoblasts were used as a source of proteins (Fig. 3b); second, in chromatin

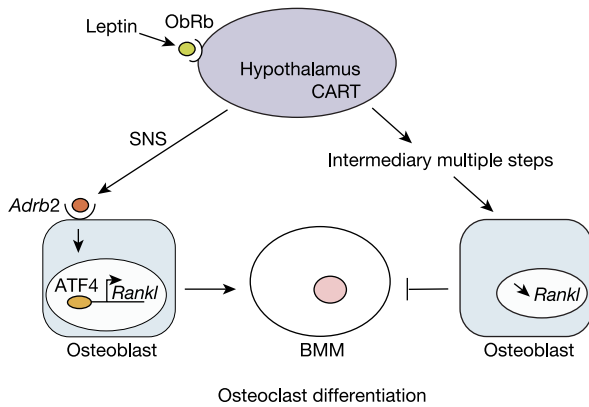


**Figure 5** Model of the neuronal control of bone resorption.

immunoprecipitation, ATF4 bound to this sequence while CREB did not, although it bound to the *c-Fos* promoter, a known target gene<sup>11</sup> (Fig. 3c). Third, in DNA cotransfection experiments, ATF4 transactivated a vector containing 6 copies of the WT but not of a mutant  $-1097^{Rankl}$  promoter element; CREB and other leucine zipper proteins did not (Fig. 3d); fourth, unlike PTH, isoproterenol did not upregulate *Rankl* expression in *Atf4*<sup>-/-</sup> osteoblasts (Fig. 3e); fifth, *Rankl* expression and osteoclast surface were decreased in *Atf4*<sup>-/-</sup> osteoblasts and bones, respectively (Fig. 3f, g).

ISO increased ATF4 transactivation function and triggered its phosphorylation, two events prevented by PKA inhibition (Fig. 3h, i). A consensus PKA phosphorylation site exists in ATF4 at serine 254. Mutating this highly conserved serine to alanine prevented PKA phosphorylation of ATF4 (Fig. 3j), and PKA forced expression enhanced ATF4 transactivation function (Fig. 3k). Conversely, ISO induced *Rankl* expression in osteoblasts lacking RSK2, another kinase regulating ATF4 function<sup>2</sup> (Fig. 3l), and failed to phosphorylate RSK2 (Supplementary Fig. 5). Thus, ATF4 phosphorylation by PKA but not by RSK2 is required for sympathetic regulation of *Rankl* expression.

ATF4 is required for sympathetic, but not PTH, regulation of *Rankl* expression, suggesting that sympathetic and PTH signalling target different subsets of osteoblasts. Indeed, *Adrb2* was expressed at its highest level in undifferentiated osteoblasts (day 0 of culture), when *Atf4* expression peaks, while *PTH receptor* expression peaked later in differentiated osteoblasts (Fig. 3m).

The biological importance of the sympathetic regulation of BR was addressed by ovariectomy of 1-month-old mice and histological analyses 4 and 12 weeks later. Ovariectomy increased osteoclast surface and Dpd urinary elimination in WT but not in *Adrb2*<sup>-/-</sup> mice. As a result, bone mass did not decrease in *Adrb2*<sup>-/-</sup> mice following gonadectomy (Fig. 4a–c). Although these results highlighted the importance of SNS integrity for the development of gonadal failure-induced bone loss, they were totally unexpected. Indeed, gonadectomized *Adrb2*<sup>-/-</sup> mice should be, in term of bone biology, a phenocopy of *ob/ob* mice that are hypogonadic and have a low sympathetic activity. Yet while *ob/ob* have an increase in BR, gonadectomized *Adrb2*<sup>-/-</sup> mice do not. This discrepancy implied that expression of gene(s) regulating BR is perturbed in *ob/ob* but not in gonadectomized *Adrb2*<sup>-/-</sup> mice.

To identify such inhibitors, we focused on genes whose expression is regulated by leptin but whose inactivation does not affect appetite or fertility. *Cart* encodes a neuropeptide whose expression in brain is increased by leptin, directly or indirectly, low in *ob/ob* mice<sup>3</sup> and normal in *Adrb2*<sup>-/-</sup> mice (Supplementary Fig. 6). *Cart*<sup>-/-</sup> mice have no overt phenotypic abnormalities<sup>12</sup>

(Supplementary Fig. 7) but displayed, in both sexes, a low bone mass phenotype at 6 months of age (Fig. 4d–e and Supplementary Fig. 8). Osteoblast numbers and bone formation rates were normal while osteoclast surface and number was nearly doubled in *Cart*<sup>-/-</sup> bones (Fig. 4d). The significant increase in urinary Dpd elimination established that *Cart*<sup>-/-</sup> osteoclasts were functional.

To determine if leptin-dependent sympathetic regulation of bone mass occurred in the absence of CART, we performed leptin ICV infusion in 1-month-old *Cart*<sup>-/-</sup> mice, a procedure increasing sympathetic signalling<sup>13</sup>. This infusion decreased bone mass and osteoclast surface more efficiently in *Cart*<sup>-/-</sup> mice than in WT littermates (Fig. 4f), demonstrating that leptin-mediated sympathetic regulation of bone mass is not impaired in the absence of CART. The more severe decrease of bone mass observed in *Cart*<sup>-/-</sup> mice following leptin ICV further established that CART is an inhibitor of BR. *Cart* is not expressed in bone cells (Fig. 4g), WT and *Cart*<sup>-/-</sup> BMMs differentiated equally well into osteoclasts, exogenous CART did not affect BMM differentiation into osteoclasts, and co-culture experiments failed to detect any *Cart*<sup>-/-</sup> cell-autonomous defect (Supplementary Fig. 9)—yet *Rankl* expression was upregulated in *Cart*<sup>-/-</sup> bones, suggesting that CART exerts its function by ultimately modulating *Rankl* signalling (Fig. 4h).

*Mc4r*<sup>-/-</sup> mice displayed an increase in hypothalamic *Cart* expression and, at 6 months of age, a HBM (Fig. 4i, j). While bone formation parameters were normal in *Mc4r*<sup>-/-</sup> mice, excluding the possibility that their HBM was secondary to a dysfunction of the leptin-dependent sympathetic regulatory loop, they displayed a marked reduction in osteoclast number. This feature provided an explanation for their HBM and was consistent with the increase in *Cart* expression. This finding suggested that the increased bone density observed in *MC4R*-deficient patients<sup>14</sup> may be caused, at least in part, by a decrease in bone resorption. The decrease in serum levels of two BR markers, Dpd and CTX, in patients lacking *MC4R* verified this hypothesis (Fig. 4k).

Thus leptin controls BR through, at least, two distinct and antagonistic pathways. On one hand, sympathetic signalling via *Adrb2* promotes osteoclast differentiation; on the other hand, CART inhibits it. Although both pathways regulate *Rankl* expression, the molecular bases of CART regulation of BR remain elusive in absence of a specific CART receptor (Fig. 5). That sympathetic regulation of bone mass occurs in the absence of CART suggests that CART uses other means to regulate bone resorption. This hypothesis is further supported by two suggestive lines of evidence: first, CART and sympathetic signalling have opposite effects on BR; second, CART (unlike sympathetic signalling) has no detectable effect on bone formation. From a biomedical perspective, the increase in bone formation and the decrease in BR characterizing *Adrb2*<sup>-/-</sup> mice add significant credence to the contention that an efficient, bone-specific, pharmacological blockade of *Adrb2* signalling would be a great asset in the management of gonadal failure-induced bone loss. □

**Methods**

**Animals, surgical procedures and histology**

Mutant mice used in these studies have been described<sup>15,16</sup>. ICV infusions and propranolol treatment were performed as described<sup>1</sup> in 2- (*Adrb2*<sup>-/-</sup>) or 1- (*Cart*<sup>-/-</sup>) month-old mice. For bone marrow transplantations, 2-month-old mice lethally irradiated with 1,100 rad in a double dose were injected with  $2 \times 10^6$  nucleated whole bone marrow cells and killed 4 months later ( $n = 5-8$  per group). Bone marrow cells were then flushed from long bones, and differentiated *in vitro* in the presence of ascorbic acid ( $50 \mu\text{g ml}^{-1}$ ) for 10 days. DNA extracted from osteoblasts was used for PCR genotyping. Immunocytochemistry studies were performed on decalcified sections using commercially available Neomycin and *Adrb2* antibodies. Bone histology and histomorphometry analyses were performed as previously described<sup>13</sup>. Twelve- $\mu\text{m}$ -resolution micro-computed tomography ( $\mu\text{CT}$ ) measurements were performed on distal femurs. Five to ten mice were analysed for each group.

## Cell and molecular studies

Osteoblasts were used<sup>3</sup> at day 0 for ISO induction. Osteoclasts were differentiated with RANKL (50 ng ml<sup>-1</sup>) and M-CSF (30 ng ml<sup>-1</sup>). Co-cultures of osteoblasts/osteoclasts were performed as described<sup>17</sup>. Following treatment, multinucleated TRAP<sup>+</sup> cells were counted in triplicate wells. For pit resorption analysis, BMMs were cultured for 3 days with M-CSF and RANKL, trypsinized, plated on dentine slices, resorption pits stained with haematoxylin and the resorbed area quantified. Gene expression was assessed by real-time PCR on osteoblasts or tissue RNA. Nuclear extracts were prepared and EMSAs were performed as described<sup>18</sup>. Chromatin immunoprecipitation assays (ChIP) were performed using primary osteoblasts. Phospho-<sup>254</sup>ATF4 antibody was generated against NLPSPGGSRGSPPK peptide in which the underlined serine was phosphorylated. Cells were treated with ISO (10 μM), PTH(1-34)(10 nM), forskolin (10 μM), PMA (phorbol 12-myristate 13-acetate, 0.2 μg ml<sup>-1</sup>) or H89 (30 μM, 30 min pre-treatment). *In vitro* kinase assays were performed as described<sup>2</sup>. COS cells were transfected with 100 ng of reporter, 30–100 ng of expression plasmids and 15 ng of RSV-β-gal reporter vector. ROS 17/2.8 were transfected as described<sup>18</sup>. Transfections were repeated at least 4 times in triplicates.

## Biochemistry

cAMP, Dpd crosslinks, creatinine urinary values, carboxy-terminal telopeptides of type-I collagen (CTX), leptin, insulin and PTH serum levels were measured using commercial kits.

## Statistical analyses

Data are expressed as mean ± s.e.m. Statistical significance was assessed by Student's test. Values were considered statistically significant at  $P < 0.05$ .

Received 15 December 2004; accepted 25 January 2005; doi:10.1038/nature03398.  
Published online 20 February 2005.

1. Takeda, S. *et al.* Leptin regulates bone formation via the sympathetic nervous system. *Cell* **111**, 305–317 (2002).
2. Yang, X. *et al.* ATF4 is a substrate of RSK2 and an essential regulator of osteoblast biology; implication for Coffin-Lowry Syndrome. *Cell* **117**, 387–398 (2004).
3. Ducy, P. *et al.* Leptin inhibits bone formation through a hypothalamic relay: A central control of bone mass. *Cell* **100**, 197–207 (2000).
4. Kristensen, P. *et al.* Hypothalamic CART is a new anorectic peptide regulated by leptin. *Nature* **393**, 72–76 (1998).
5. Chruscinski, A. J. *et al.* Targeted disruption of the beta2 adrenergic receptor gene. *J. Biol. Chem.* **274**, 16694–16700 (1999).
6. Thomas, S. A., Matsumoto, A. M. & Palmiter, R. D. Noradrenaline is essential for mouse fetal development. *Nature* **374**, 643–646 (1995).
7. Friedman, J. M. & Halaas, J. L. Leptin and the regulation of body weight in mammals. *Nature* **395**, 763–770 (1998).
8. Dominici, M. *et al.* Hematopoietic cells and osteoblasts are derived from a common marrow progenitor after bone marrow transplantation. *Proc. Natl Acad. Sci. USA* **101**, 11761–11766 (2004).
9. Teitelbaum, S. L. & Ross, F. P. Genetic regulation of osteoclast development and function. *Nature Rev. Genet.* **4**, 638–649 (2003).
10. Lacey, D. L. *et al.* Osteoprotegerin ligand is a cytokine that regulates osteoclast differentiation and activation. *Cell* **93**, 165–176 (1998).
11. Berkowitz, L. A., Riabowol, K. T. & Gilman, M. Z. Multiple sequence elements of a single functional class are required for cyclic AMP responsiveness of the mouse *c-fos* promoter. *Mol. Cell. Biol.* **9**, 4272–4281 (1989).
12. Asnicar, M. A. *et al.* Absence of cocaine- and amphetamine-regulated transcript results in obesity in mice fed a high caloric diet. *Endocrinology* **142**, 4394–4400 (2001).
13. Satoh, N. *et al.* Sympathetic activation of leptin via the ventromedial hypothalamus: leptin-induced increase in catecholamine secretion. *Diabetes* **48**, 1787–1793 (1999).
14. Orwoll, B., Bouxsein, M. L., Marks, D. L., Cone, R. D. & Klein, R. F. in *ORS/AAOS Presentations 2003, 71st Annual Meeting of the AAOS (ORS, San Francisco, CA, 2004)*.
15. Rohrer, D. K., Chruscinski, A., Schauble, E. H., Bernstein, D. & Kobilka, B. K. Cardiovascular and metabolic alterations in mice lacking both beta1- and beta2-adrenergic receptors. *J. Biol. Chem.* **274**, 16701–16708 (1999).
16. Huszar, D. *et al.* Targeted disruption of the melanocortin-4 receptor results in obesity in mice. *Cell* **88**, 131–141 (1997).
17. Takahashi, N. *et al.* Osteoblastic cells are involved in osteoclast formation. *Endocrinology* **123**, 2600–2602 (1988).
18. Ducy, P. & Karsenty, G. Two distinct osteoblast-specific cis-acting elements control expression of a mouse osteocalcin gene. *Mol. Cell. Biol.* **15**, 1858–1869 (1995).

**Supplementary Information** accompanies the paper on [www.nature.com/nature](http://www.nature.com/nature).

**Acknowledgements** We thank T. Townes and A. Hanauer for *Atf4* and *Rsk2*−/− mice, A. Hanauer and M. Montminy for RSK2 and CREB antibodies, M. Huelskamp and D.A. Horst for Dpd and CTX measurements, P. Ducy for suggestions and critical readings of the manuscript, and L. Li for technical assistance. This work was supported by grants from NIH, NSBRI and CNRC (G.K., F.E.), Arthritis Foundation (S.T.) and Children's Brittle Bone Foundation (X.Y.).

**Competing interests statement** The authors declare that they have no competing financial interests.

**Correspondence** and requests for materials should be addressed to G.K. (karsenty@bcm.tmc.edu).

# Recognition of bacterial glycosphingolipids by natural killer T cells

Yuki Kinjo<sup>1</sup>, Douglass Wu<sup>2</sup>, Gisen Kim<sup>1</sup>, Guo-Wen Xing<sup>2</sup>, Michael A. Poles<sup>3,4</sup>, David D. Ho<sup>4</sup>, Moriya Tsuji<sup>4,5</sup>, Kazuyoshi Kawahara<sup>6\*</sup>, Chi-Huey Wong<sup>2</sup> & Mitchell Kronenberg<sup>1</sup>

<sup>1</sup>Division of Developmental Immunology, La Jolla Institute for Allergy and Immunology, San Diego, 10355 Science Center Drive, San Diego, California 92121, USA

<sup>2</sup>Department of Chemistry and Skaggs Institute for Chemical Biology, The Scripps Research Institute, 10550 North Torrey Pines Road, La Jolla, California 92037, USA

<sup>3</sup>Department of Medicine, Division of Gastroenterology, New York University School of Medicine, 550 First Avenue, New York, New York 10016, USA

<sup>4</sup>Aaron Diamond AIDS Research Center, The Rockefeller University, 455 First Avenue, New York, New York 10016, USA

<sup>5</sup>Department of Medical and Molecular Parasitology, New York University School of Medicine, 341 E. 25th Street, New York, New York 10010, USA

<sup>6</sup>The Kitasato Institute, Minato-ku, Tokyo 108-8642, Japan

\* Present address: Department of Applied Material and Life Science, College of Engineering, Kanto Gakuin University, Yokohama 236-8501, Japan

Natural killer T (NKT) cells constitute a highly conserved T lymphocyte subpopulation that has the potential to regulate many types of immune responses through the rapid secretion of cytokines<sup>1,2</sup>. NKT cells recognize glycolipids presented by CD1d, a class I-like antigen-presenting molecule. They have an invariant T-cell antigen receptor (TCR) α-chain, but whether this invariant TCR recognizes microbial antigens is still controversial. Here we show that most mouse and human NKT cells recognize glycosphingolipids from *Sphingomonas*, Gram-negative bacteria that do not contain lipopolysaccharide<sup>3–5</sup>. NKT cells are activated *in vivo* after exposure to these bacterial antigens or bacteria, and mice that lack NKT cells have a marked defect in the clearance of *Sphingomonas* from the liver. These data suggest that NKT cells are T lymphocytes that provide an innate-type immune response to certain microorganisms through recognition by their antigen receptor, and that they might be useful in providing protection from bacteria that cannot be detected by pattern recognition receptors such as Toll-like receptor 4.

A glycosphingolipid, known as KRN 7000 or α-galactosyl ceramide (α-GalCer), was isolated from a marine sponge in a screen for compounds that could prevent tumour metastases to the liver of mice<sup>6</sup>. This activity was subsequently shown to be caused by the CD1d-mediated stimulation of NKT cells with an invariant Vα14 (Vα14i) TCR rearrangement<sup>7</sup>. Although in mice these form the majority of T cells that also express natural killer receptors, such as NK1.1, to distinguish them from other T cells that express natural killer receptors we refer to them as Vα14i NKT cells. The reactivity of NKT cells for α-GalCer presented by CD1d is unusually conserved, because mouse Vα14i NKT cells recognize α-GalCer presented by heterologous human CD1d<sup>8</sup>, and human NKT cells with an invariant rearrangement of Vα24 (Vα24i), the orthologue of mouse Vα14, recognize α-GalCer presented by mouse CD1d<sup>8</sup>. Very few other examples of this type of interspecies cross-reactivity for T cells exist, indicating that this specificity and the conserved, invariant Vα (Vαi) rearrangements required for it might be particularly important. Although glycosphingolipids are widely distributed, α-GalCer is unusual because it has an α linkage of the 1' carbon of the sugar to the 1 carbon of the sphingosine base. However, in nearly all other glycosphingolipids the bond connecting the sugar to the lipid is in the β anomeric form, but this β form is not antigenic. It is unlikely that mice and humans have T-cell